Available online at www.sciencedirect.com

SCIENCE DIRECT®

Remote Sensing of Environment 98 (2005) 201 – 211

Remote Sensing of Environment

www.elsevier.com/locate/rse

Leaf BRDF measurements and model for specular and diffuse components differentiation

Laurent Bousquet [a,c,*], Sophie Lachérade [a,d], Stéphane Jacquemoud [a,c], Ismaël Moya [b]

[a] Université Paris 7 - Denis Diderot, Laboratoire Environnement et Développement, CP 7071, 2 place Jussieu, 75251 Paris Cedex 5, France
[b] Centre National de la Recherche Scientifique, Laboratoire pour l'Utilisation du Rayonnement Electromagnétique, Université de Paris-Sud, 91405 Orsay Cedex, France
[c] Institut de Physique du Globe de Paris, Géodésie et Gravimétrie, CP 89, 4 place Jussieu, 75252 Paris Cedex 5, France
[d] Office National d'Etudes et de Recherches Aérospatiales, Département d'Optique Théorique et Appliquée, 2 avenue Edouard Belin, 31055 Toulouse Cedex 4, France

Received 12 April 2005; received in revised form 11 July 2005; accepted 12 July 2005

Abstract

This paper aims to link the spectral and directional variations of the leaf Bidirectional Reflectance Distribution Function (BRDF) by differentiating specular and diffuse components. To do this, BRDF of laurel (*Prunus laurocesarus*), European beech (*Fagus silvatica*) and hazel (*Corylus avellana*) leaves were measured at 400 wavelengths evenly spaced over the visible (VIS) and near-infrared (NIR) domains (480–880 nm) and at 400 source-leaf-sensor configurations. Measurement analysis suggested a spectral invariance of the specular component, the directional shape of which was mainly driven by leaf surface roughness. A three-parameter physically based model was fitted on the BRDF at each wavelength, confirming the spectral invariance of the specular component in the VIS, followed by a slight deterioration in the NIR. Due to this component, the amount of reflected light which did not penetrate into the leaf, could be considered as significant at wavelengths of chlorophyll absorption. Finally, by introducing the PROSPECT model, we proposed a five-parameter model to simulate leaf spectral and bidirectional reflectance in the VIS–NIR.

Keywords: Leaf optics; BRDF; Photogoniometer; Model

1. Introduction

Plant leaves are the main organs intercepting the photosynthetic active radiation (PAR) from 400 to 800 nm. Their optical properties vary with the wavelength and the measurement configuration: the spectral and directional distributions of incoming and outgoing light can be exploited to get information about leaf biochemistry and anatomy. Most papers have focused on the leaf spectral reflectance and transmittance in connection with their chlorophyll, water, cellulose, nitrogen, etc., contents. From such measurements, Allen et al. (1969) estimated the effective refractive index of corn by inverting a plate model based on geometric optics. Jacquemoud and Baret (1990) further developed the PROSPECT model, which led to precise water, chlorophyll and dry matter content estimation for various kinds of leaves. Woolley (1971) was among the first to take interest in the spatial distribution of reflected light on philodendron, maize and soybean leaves: he distinguished diffuse from specular components and showed that the latter was significant contrary to the usual assumptions in most canopy reflectance models. Breece and Holmes (1971) scanned nineteen narrow wavebands, observing that the specular component was relatively more important in strong absorption domains. Finally Brakke et al. (1989) related the characteristics of those two components to leaf anatomy but their measurements were restricted to a single wavelength.

* Corresponding author. Université Paris 7 - Denis Diderot, Laboratoire Environnement et Développement, CP 7071, 2 place Jussieu, 75251 Paris Cedex 5, France.
E-mail address: lbousque@ccr.jussieu.fr (L. Bousquet).

0034-4257/$ - see front matter © 2005 Elsevier Inc. All rights reserved.
doi:10.1016/j.rse.2005.07.005

Previous studies on leaf optical properties emphasized that the distinction between specular and diffuse reflection was required to improve the link between biophysical parameters and remote sensing data. It is therefore relevant to separate these two components in plant leaf reflection because they carry different information. On the one hand, the diffuse component results from multiple scattering of light within the leaf. Its angular distribution is quite isotropic and thus does not carry any exploitable information while its spectral variation depends on leaf biochemistry and thus can be used to estimate the amount of the leaf constituents. On the other hand, the specular component results from the single regular scattering at the leaf surface. It consequently depends on surface biophysical properties. Its magnitude and angular distribution should permit the estimation of the refractive index or the roughness of the epidermis/cuticle layer. Conversely, its spectral variation should not be or very little affected by constituents like chlorophyll in the VIS.

To separate specular reflectance from diffuse reflectance, polarization measurements are classically used. This is because surface scattering polarizes the incident light, while the multiple scattering within the leaf mesophyll, created by the many discontinuities between the air spaces and the cell walls, does not. Vanderbilt and Grant (1986) developed an optical device measuring polarization effects for this purpose. With this technique, Brakke (1994) showed that the specular component was almost the same in the VIS–NIR whereas the diffuse component decreased in the VIS. The directional repartition of the reflected light as a function of wavelength should confirm this experimental result but it has not been previously studied because appropriate datasets were lacking.

Since BRDF are measured, models have been developed to fit them. Ward (1992) and Brakke et al. (1989) proposed simple equations leading to the estimation of empirical parameters. To go further in the interpretation of the signal, physically based models are required. The concepts of Bidirectional Reflectance and Transmittance Distribution Functions (BRDF and BTDF) detailed in Nicodemus et al. (1977) capture the spectral and directional variations of optical properties. It is now widely used in the remote sensing community and also in the field of computer-generated pictures. Most surface BRDF models with physical input parameters are seen as the sum of a specular and a diffuse component. The simplest way to describe the diffuse component is the Lambert model which assumes that light is isotropically reflected, which, of course, is an idealistic behaviour. Torrance and Sparrow (1967) laid the foundations for more realistic surface BRDF models. They treated the surface as small facets, however much larger than the wavelength and applied the laws of geometric optics to derive the corresponding BRDF. Cook and Torrance (1981) and Oren and Nayar (1995) extended this work with accurate expressions for the specular and diffuse components. Govaerts et al. (1996) and Baranoski and Rokne (2004) built models for use with ray tracing techniques. High computing requirements however have prevented inverting such models.

This paper aims to link the spectral and directional variations of leaf BRDF by differentiating specular and diffuse components. To do this we measured leaf BRDF at 400 wavelengths evenly spaced over the VIS–NIR from 480 to 880 nm and at 400 source-leaf-sensor configurations. We first analyzed both specular and diffuse components as they appeared in our measurements and tested the influence of leaf surface roughness on the BRDF pattern. Then we modeled the observed BRDF as the sum of a diffuse and a specular component to study their spectral variation and we estimated the amount of light that really penetrated into the leaf. Finally we gave an interesting perspective to such a model for leaf surface properties estimation and leaf BRDF modeling with a minimum number of parameters.

2. BRDF measurements

This section presents the main physical quantities used in this study and describes the device and campaign for leaf BRDF measurements.

2.1. Definitions

The Bidirectional Reflectance Distribution Function (BRDF) characterizes the bidirectional reflectance properties of an object. It is defined as the ratio of its radiance R to the irradiance I:

$$\mathrm{BRDF}(\lambda,\theta_s,\varphi_s,\theta_v,\varphi_v)=\frac{R(\lambda,\theta_s,\varphi_s,\theta_v,\varphi_v)}{I(\lambda,\theta_s,\varphi_s)} \quad (1)$$

where all the notations and units are specified in Table 1. The azimuth illumination angle φ_s is conventionally equal to zero and will not be mentioned. Note that the Bidirectional Reflectance Factor (BRF) also commonly used in remote sensing equals π times the BRDF. An important related quantity is the Directional Hemispheric Reflectance Factor (DHRF) defined as:

$$\mathrm{DHRF}(\lambda,\theta_s)=\int_0^{2\Pi}\int_0^{\Pi/2}\mathrm{BRDF}(\lambda,\theta_s,\theta_v,\varphi_v)\cos\theta_v\sin\theta_v\,\mathrm{d}\theta_v\,\mathrm{d}\varphi_v. \quad (2)$$

2.2. Measurement device

Measurements were performed with a spectro-photo-goniometer developed by the Institut National de la Recherche Agronomique (Combes, 2002), the University of Paris 7, and the LURE/CNRS. This device which is fully described in a forthcoming paper was specifically designed for leaf BRDF/BTDF measurements but has also been used for BRDF measurements of man-made, opaque materials like slates. We used a halogen light source producing

Table 1
Notations

Symbol	Quantity	Unit (symbol)
$\vec{L}$	Illumination direction	None
$\vec{V}$	Viewing direction	None
$\vec{N}$	Normal to the sample	None
$\vec{H}$	Normal to the facet	None
λ	Wavelength	Nanometer (nm)
θ_s	Illumination (solar) zenith angle (in spherical coordinates)	Degree (°)
φ_s	Illumination (solar) azimuth angle (in spherical coordinates)	Degree (°)
θ_v	Viewing zenith angle (in spherical coordinates)	Degree (°)
φ_v	Viewing azimuth angle (in spherical coordinates)	Degree (°)
θ_a	Half of the phase angle between $\vec{L}$ and $\vec{V}$	Degree (°)
α	Angle between $\vec{N}$ and $\vec{H}$	Degree (°)
R	Radiance	Watt per square meter per steradian (W m^{-2} sr^{-1})
I	Irradiance	Watt per square meter (W m^{-2})
BRDF/BTDF	Bidirectional reflectance/transmittance distribution function	Unit per steradian (sr^{-1})
DHRF	Directional hemispherical reflectance factor	None
$d\Omega$	Solid angle	Steradian (sr)
k_L	Lambert parameter of the BRDF model	None
n	Refractive index	None
σ	Leaf surface roughness parameter	None
N	Leaf structure parameter	None
C_{ab}	Leaf chlorophyll content	µg cm^{-2}
C_m	Leaf dry matter content	g cm^{-2}

unpolarized radiation in the VIS–NIR, which was carried to an illumination arc by an optical fiber. The zenith illumination angle could be set to 8°, 21°, 41°, and 60°. The sample holders were designed for leaves and reflectance standards of about 30 mm wide. Seven detectors in different viewing directions were arranged along a fixed reception arc. By moving together the illumination arc and the sample holder, one could obtain 98 different observation directions. The radiometric measurements ranged from 480 to 880 nm with a 1 nm step. Accurate derivation of measurement error has not been driven.

2.3. Measurement campaign

Measurements were made during spring 2003 on leaf species listed in Table 2. As surface effects are thought to be of great importance for BRDF pattern, species were selected to display various kinds of surface structure. Cherry laurel with a thick smooth cuticle on the adaxial face was very bright to the naked eye. In the opposite extreme, hazel presented a diffuse aspect because of its hairy surface. European beech, one of the most widespread tree species in Europe, was intermediate in leaf characteristics. The other leaves were selected for their economic interest like maple, a high-value ornamental plant, or like green bean, because it has been the subject of experimental measurements in our laboratories. Brakke et al. (1989) has shown differences in the BRDF of adaxial and abaxial faces. Measurements over both faces of several leaf samples of each species have been made to address this difference and the intra-species variability. A full BRDF acquisition corresponding to 4 illumination directions, 98 viewing directions, and 400 wavelengths took less than an hour after the leaf was removed from the plant. We assumed a minimal pigment and anatomy degradation, i.e. unchanged leaf optical properties in the VIS–NIR.

The size of the lit and viewed area of the leaf may influence the measurement of the leaf BRDF. Regardless of illumination and viewing directions, we set the observed area of the leaf to be smaller than the lit one. As we wished to avoid major veins on the leaf, it was necessary for the lit area to be smaller than a few square centimeters. However, it also needed to be large enough to average the properties of the mesh constituted by the leaf areolaes, which are the spaces enclosed by anastomosing veinlets. Wylie (1943) measured the area of areolae in more than ten species and found an average area of 0.06 mm^2. An observed area one hundred times greater, i.e., 6 mm^2, thus guarantees sufficient averaging of the optical properties for a mesh of this size. The lit and viewed areas of the leaf were set to satisfy these constraints. Mechanical defects affected the localization of the viewed area at grazing angles and caused a signal loss beyond $\theta_v = 70°$ so that the corresponding BRDF values were not accounted for in this study although they were

Table 2
Description of the dataset

Sample	Description	Type of measurement
Hazel (*Corylus avellana*)	Downy and undulating	Adaxial and abaxial BRDF
Cherry laurel (*Prunus laurocesarus*), young leaf	Clear green, flexible leave	Adaxial and abaxial BRDF
Cherry laurel (*Prunus laurocerasus*), old leaf	Dark green, rigid	Adaxial and abaxial BRDF
European beech (*Fagus silvatica*)	Very undulating	Adaxial and abaxial BRDF
Maple (*Acer pseudoplatanus*), young leaf	Bright and undulating	Adaxial and abaxial BRDF
Maple (*Acer pseudoplatanus*), old leaf	Mat and flat	Adaxial and abaxial BRDF
Maple (*Acer pseudoplatanus*), old leaf	Green adaxial and purple abaxial faces	Adaxial and abaxial BRDF
Green bean (*Phaseolus vulgaris* var. contender)	Slightly undulating	Adaxial BRDF

plotted. Effects of the geometry of the incident and reflected light beams have not been studied.

Measuring leaf BRDF, one has to account for their undulating shape and surface features that are responsible for several roughness scales. The latter must be compared with the length of the observed surface, about 1 cm in the present work. When below this the roughness is intrinsic to the sample and may be modeled as described in the following section. However it may tilt the average plane of the observed surface in the sample holder. As a result the observed specular reflection may not be in the expected direction. We selected samples with specular peaks in the principal plane defined as the plane of the incident light beam and the normal to the sample holder.

3. Analysis of measured BRDF

In this section we aim to distinguish specular from diffuse reflection patterns directly in the measured BRDF and to study the impact of various leaf surface roughnesses on the directional shape of the BRDF.

3.1. Discrimination of specular and diffuse reflections in the laurel BRDF

Because of a thick smooth cuticle and high chlorophyll content, the laurel leaf is the most suitable for the observation of a strong white specular peak on a green diffuse background caused by chlorophyll absorption. The 98 viewing directions should permit the localization of the specular peak and the 400 wavelengths, correspondingly, the study of its spectral composition. Fig. 1 shows the BRDF of laurel at 550, 670, and 780 nm. The BRDF are plotted for a given wavelength (λ) and a given illumination direction (θ_s) in polar coordinates (r,θ), respectively, equal to (θ_v,φ_v). Incident direction is represented by a star. Thus one plot shows the variation of the BRDF over the whole hemisphere. Directions of experimental data acquisition are marked by dots. The other values have been interpolated for this representation. The first waveband corresponds to the maximum leaf reflection in the visible domain (green), the second one to a minimum reflection (red), and the third one lies in the near-infrared domain where reflection reaches a high plateau (due to minimum absorption). The incidence angle θ_s is set to 60° to enhance the specular reflection at all wavelengths.

The BRDF pattern consists of a thin high peak in the specular direction and a uniform background in all other viewing directions. The peak maximum is about 1.2 sr^{-1} and may vary up to 10% with wavelength. The intensity of the background is smaller than 0.1 sr^{-1} in the VIS and about 0.2 sr^{-1} in the NIR. The peak in the BRDF is thus identified as almost pure specular reflection. In comparison, although diffuse reflection appears very low, it becomes predominant once integrated over the whole hemisphere. Indeed, the specular peak reaches high intensities but remains confined within a small solid angle. The laurel DHRF (Eq. (2)) which has been evaluated for θ_s=60° by numerical summation is about 0.1 in the red, 0.2 in the green, and 0.5 in the near-infrared. If the contribution of

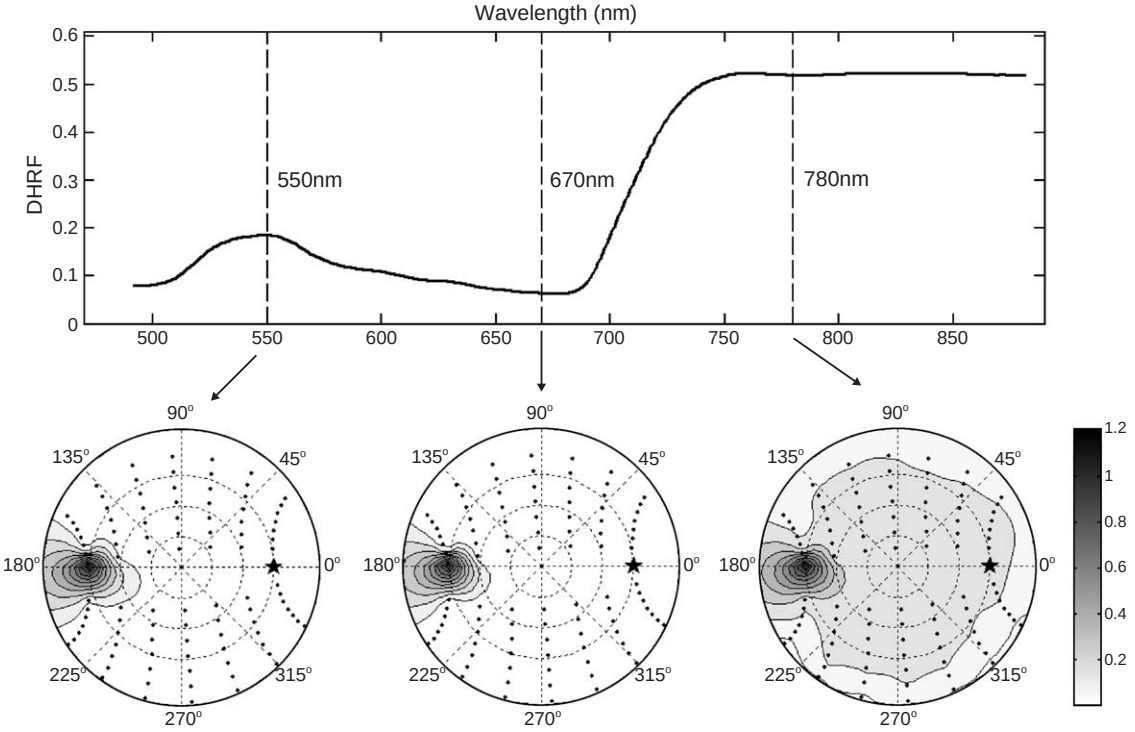

Fig. 1. Laurel DHRF (top) and BRDF (bottom) calculated for θ_s=60° at 550 (left), 670 (middle), and 780 nm (right). The bar scale is the same for the three plots.

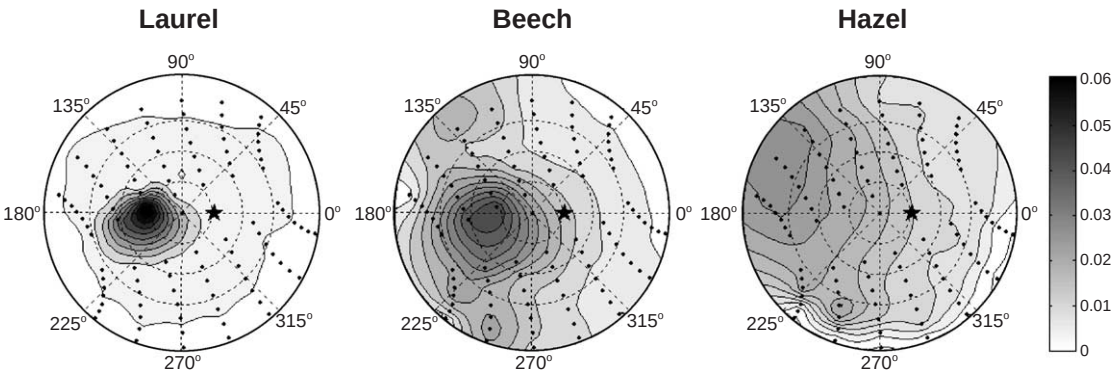

Fig. 2. BRDF of adaxial leaf faces of laurel (left), European beech (middle), and hazel (right) for θ_s=21° and λ=680 nm. The bar scale is the same for the three plots.

specular reflection to the DHRF is constant, it must be less than 0.1 DHRF unit. This could still represent the half or more of the reflected light in the visible domain. In the next section, the use of a BRDF model will enable us to accurately quantify this contribution.

3.2. Influence of surface roughness

Differences in BRDF patterns are thought to come from specular reflection. For wavelengths of strong absorption, for instance 680 nm where chlorophyll is at full absorption, specular reflection is highlighted when compared to diffuse reflection, as previously noticed by Walter-Shea et al. (1989). The experimental BRDF of the three leaf species, beech, laurel, and hazel, are presented in Fig. 2 to illustrate different BRDF magnitudes and patterns. All leaves showed forward scattering whereas no backscattering was observed. With its thick cuticle creating a very smooth surface on the adaxial face, laurel displayed a thin high BRDF peak localized in the specular direction. Hazel was much more Lambertian, with a maximum reflectance measured at very high viewing angles. This may be due to its hairy surface and undulated shape. Finally, beech showed an intermediate BRDF pattern with a lower reflectance and peak localized over a larger area between 20° and 40°. As noticed by Woolley (1971) and Walter-Shea et al. (1989), the maxima of BRDF may appear at a greater angle than for a mirror-like reflection. This effect which is due to leaf roughness (Torrance and Sparrow, 1967) tends to vanish when the latter decreases. As the zenith illumination angle increases, the three samples become more specular and the BRDF peak becomes narrower and higher. For a 60° illumination angle, BRDF maxima are 1.1 sr^{-1} for laurel, 0.29 sr^{-1} for beech and 0.14 sr^{-1} for hazel. The differences between the three samples remain such that differentiation based upon their BRDF shape is possible.

4. Modeling of leaf BRDF and applications

Because they contain both a spectral and a bidirectional dimension, our BRDF measurements allowed us to identify specular and diffuse reflection components and to look at surface roughness effects. In this section we propose a BRDF model defined as the sum of diffuse and specular components and we test its ability to fit the experimental measurements. It will permit to assess the spectral invariance of the specular component and to evaluate the amount of reflected light that did not penetrate into the leaf. We also investigate perspectives for the estimation of leaf surface properties and propose a simple way to represent leaf BRDF in the VIS–NIR with only five parameters.

4.1. Derivation of a geometric optics BRDF model

The BRDF is assumed to be the sum of the diffuse and specular components, namely $BRDF_{diff}$ and $BRDF_{spec}$:

$$BRDF = BRDF_{diff} + BRDF_{spec}. \quad (3)$$

We wish to derive a simple and general expression of leaf BRDF that can be used for model inversion or for plant canopy reflectance simulations. The diffuse component represents the fraction of reflected light which is not single specular reflection at the leaf surface. We assume Lambertian behaviour and a strong dependence on wavelength so that $BRDF_{diff}$ may be written:

$$BRDF_{diff}(\lambda, \theta_s, \theta_v, \varphi_v) = \frac{k_L(\lambda)}{\pi} \quad (4)$$

where $1/\pi$ is the BRDF of a perfect Lambertian scatterer and $k_L(\lambda)$ is the Lambert coefficient. Note that the diffuse component does not vary with the incidence angle. To model the shape of the specular component, one needs to consider the leaf surface as a rough interface between air and leaf material. A recurrent modeling approach for rough surfaces assumes that they are composed of a multitude of facets. Among the last ones, some reflect light specularly from the illumination direction $\vec{L}$ to the viewing direction $\vec{V}$ (Fig. 3). Torrance and Sparrow (1967), Cook and Torrance (1981), and Oren and Nayar (1995) derived various BRDF expressions based on this approach. Consider a plane surface of area S illuminated by a parallel light beam. At a smaller scale this surface is made of N_f tilted mirror-like

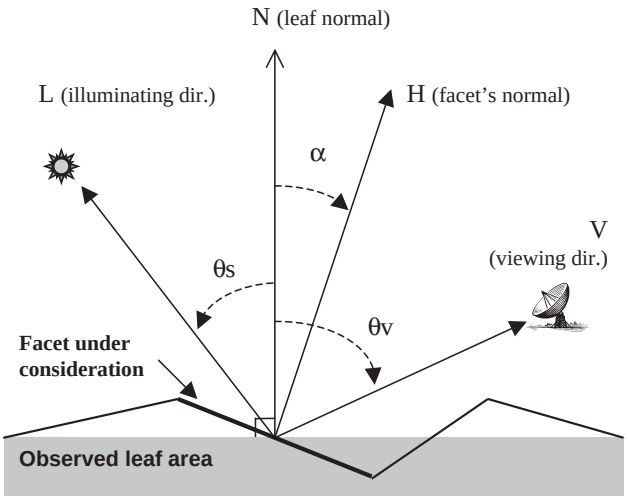

Fig. 3. Notations for the main directions and angles.

facets of the same area S_f. Facets are identified by the direction of their normal (α, Φ). The probability to find a facet (α, Φ) in the solid angle $d\Omega = \sin\alpha d\alpha d\Phi$ is $D(\alpha, \Phi)d\Omega$ where the probability density function $D(\alpha, \Phi)$ is normalized to unity. The area of the plane surface is linked to the facet area by the following expression:

$$S = \int_0^{2\Pi}\int_0^{\Pi/2} \cos\alpha N_f D(\alpha, \Phi)\sin\alpha d\alpha d\Phi. \quad (5)$$

We calculate the BRDF for an illumination direction (θ_s, φ_s) and a viewing direction (θ_v, φ_v). Only facets producing specular reflection between these two directions are accounted for. The amount of reflected light by a single facet is given by the Fresnel factor $F(n, \theta_a)$ which depends on the refractive index n of leaf surface material and the angle of incidence θ_a between the normal to the facet and the illumination direction. Oren and Nayar (1995) detailed the geometrical effects of multiple specular reflections and mutual facet masking or shadowing which led to several conditional expressions. For simplicity's sake we used the approach of Cook and Torrance (1981) which assumes a multiplying geometrical attenuation factor G depending only on the illumination and viewing directions. This yields to the following expression (readers are invited to refer to Torrance and Sparrow (1967) for details):

$$BRDF_{spec}(\lambda, \theta_s, \theta_v, \Phi_v) = \frac{F(n, \theta_a)D(\alpha, \Phi)G(\theta_s, \theta_v, \Phi_v)}{4\cos\theta_s\cos\theta_v} \times \frac{S_f N_f}{S} \quad (6)$$

where:

$$G(\theta_s, \theta_v, \varphi_v) = \min(1, E_1, E_2) \quad (7)$$

with $E_1 = \frac{2\cos\alpha\cos\theta_v}{\cos\theta_a}$ and $E_2 = \frac{2\cos\alpha\cos\theta_s}{\cos\theta_a}$. The angles θ_a and α are derived from basic geometry as $\cos\alpha = \frac{\cos\theta_s + \cos\theta_v}{2\cos\theta_a}$ and $\cos 2\theta_a = \cos\theta_s\cos\theta_v + \sin\theta_s\sin\theta_v\cos\varphi_v$.

The Fresnel factor $F(n, \theta_a)$ drives the amount of light reflected at the boundary between air and leaf material. The cuticle which coats the leaf epidermal cells (Juniper and Jeffree, 1983) is assumed to be a low absorbing medium compared to the leaf interior. Thus its absorption can be neglected and its refractive index assumed real. The Fresnel factor is calculated for a plane dielectric boundary between two semi-infinite media and unpolarized light:

$$F(n, \theta_a) = \frac{1}{2}\left(\frac{g - \cos\theta_a}{g + \cos\theta_a}\right)^2\left[1 + \left(\frac{\cos\theta_a(g + \cos\theta_a) - 1}{\cos\theta_a(g - \cos\theta_a) + 1}\right)^2\right] \quad (8)$$

with $g^2 = n^2 + \cos^2\theta_a - 1$. When absorption cannot be neglected, this factor is expressed as a function of the real and imaginary parts of the complex refractive index of the medium.

The probability density function $D(\alpha, \Phi)$ used in Torrance and Sparrow (1967) and Oren and Nayar (1995) is a Gaussian distribution of the variable α leading to difficulties in evaluation of integral forms. In order to represent a wide panel of surfaces and to make the integral of S calculable, we used the expression of D proposed by Cook and Torrance (1981) and which depends on a roughness parameter σ:

$$D(\alpha, \Phi, \sigma) = \frac{c}{\sigma^2\cos^4\alpha}\exp\left(-\frac{\tan^2\alpha}{\sigma^2}\right). \quad (9)$$

The normalization factor c is not present in their work but it cancels in the final expression of $BRDF_{spec}$. Note that the azimuth angle Φ does not affect the probability to find a facet (α, Φ). This expression permits the calculation of the factor $(S_f N)/S$ in Eq. (6) yielding to an expression independent of the roughness parameter σ.

The final BRDF expression for $BRDF_{spec}$ is:

$$BRDF_{spec}(n, \sigma, \theta_s, \theta_v, \varphi_v) = \frac{F(n, \theta_a)G(\theta_s, \theta_v, \varphi_v)}{2\pi^2\cos\theta_s\cos\theta_v} \times \frac{e^{-\tan^2\alpha/\sigma^2}}{\sigma^2\cos^4\alpha}. \quad (10)$$

Using this expression for leaves, one should keep in mind that it is just a simplification since other leaf surface features like trichomes of hairy leaves (Fuhrer et al., 2004) may involve other optical phenomena like diffraction. In the absence of such surface features, the facets of the BRDF model may correspond to the leaf areolae defined as the spaces enclosed by anastomosing veinlets.

The simulated BRDF depends on the refractive index n via the Frenel factor, the behaviour of which is well-

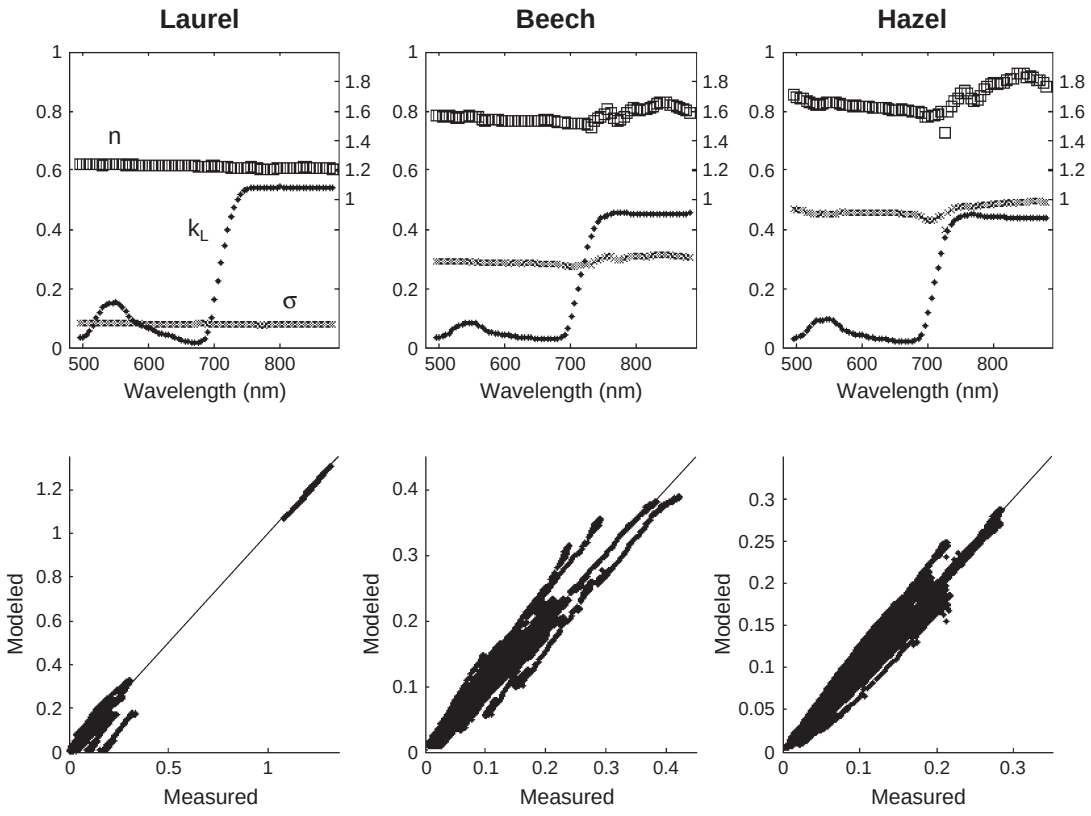

Fig. 4. Three-parameter model inversion at each wavelength for laurel (left), beech (middle), and hazel (right). Top: parameter values as a function of wavelength. Scale for k_L and σ on the left, for n on the right. Bottom: measured vs modeled BRDF.

known, and on the roughness parameter via the probability density function D. Provided that the roughness parameter σ is smaller than 0.7, the probability to find a facet with the tilt α decreases when α increases. For a given n, $\sigma<0.1$ leads to a thin high specular peak, $\sigma\approx0.3$ to a much wider and weaker peak, and $\sigma>0.5$ to a forward scattering rather than a specular peak. To study the effects of n and σ on the reflected light over the whole hemisphere we derived the DHRF due to $BRDF_{spec}$, namely $DHRF_{spec}$. For n equal to 1.4 and σ increasing from 0.1 to 0.5, $DHRF_{spec}$ remains unchanged for incidence angles lower than 30° and decreases with σ especially as the incidence angle is large. For $\sigma=0.25$ and n increasing from 1.2 to 1.8, $DHRF_{spec}$ does not change for large incidence angles and increases with n especially at small incidence angles. Thus increasing the roughness parameter σ tends to reduce $DHRF_{spec}$ at large incidence angles while increasing the refractive index n tends to increase $DHRF_{spec}$ at small incidence angles.

4.2. Inversion of the model for each wavelength of the measured BRDF

The BRDF model has three input parameters (k_L,n, and σ) and we experimentally measured the shape of the BRDF of several plant leaves at 400 wavelengths. Thus we can retrieve these parameters at each wavelength separately by minimizing the merit function χ^2 defined as:

$$\chi^2(\lambda)=\sum_{\theta_s,\theta_v,\varphi_v}\left(\mathrm{BRDF}_{\mathrm{measured}}-\mathrm{BRDF}_{\mathrm{modeled}}\right)^2. \qquad (11)$$

Because data acquired at viewing zenith angles higher than 70° invite criticism as above-mentioned, only 65 viewing directions of the 98 measured were used, which represent 260 reflectances for each sample at each of the 400 wavelengths. The optimization has been constrained by fixing the lower and upper parameter bounds. For one inversion, the initial parameter set is the same for all the samples and all the wavelengths. Several inversions performed with various initial parameter sets led to similar results. Results are presented in Fig. 4 for the parameter set shown in Table 3. Measured vs modeled BRDF values are in good agreement. Fig. 5 shows the measured and modeled BRDF at wavelengths of mini-

Table 3
Parameter sets for model inversion

	k_L	n	σ
Lower bound	0.01	1.1	0.01
Upper bound	0.99	5	1
Initial value	0.3	1.47	0.3

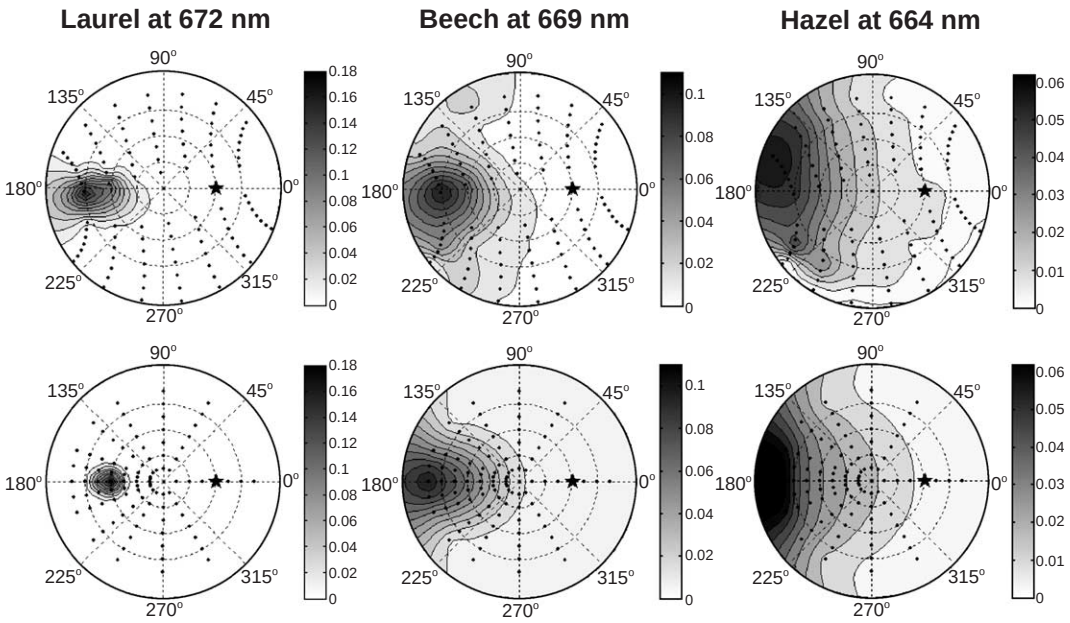

Fig. 5. Measured (top) and modeled (bottom) BRDF for θ_s=41° at wavelengths of minimum reflection.

mum reflection. They reveal very similar directional shapes. This proves the ability of the model to fit the directional variations of the reflected light that did not penetrate into the leaf.

4.3. Spectral invariance of the specular component

The parameters n and σ vary quite slowy over the whole measured spectrum compared to k_L. In the VIS, the variations ((max−min)/mean) of n are about 2% for laurel, 5% for beech, and 10% for hazel. σ varies by about 8%, 7%, and 9%, respectively. These variations increase in the NIR, almost reaching 25% for the refractive index of hazel. Note that the spectral variation of n in the NIR has the same pattern for beech and hazel. The spectral invariance of the specular component can consequently be considered as a good approximation in the VIS that deteriorates in the NIR.

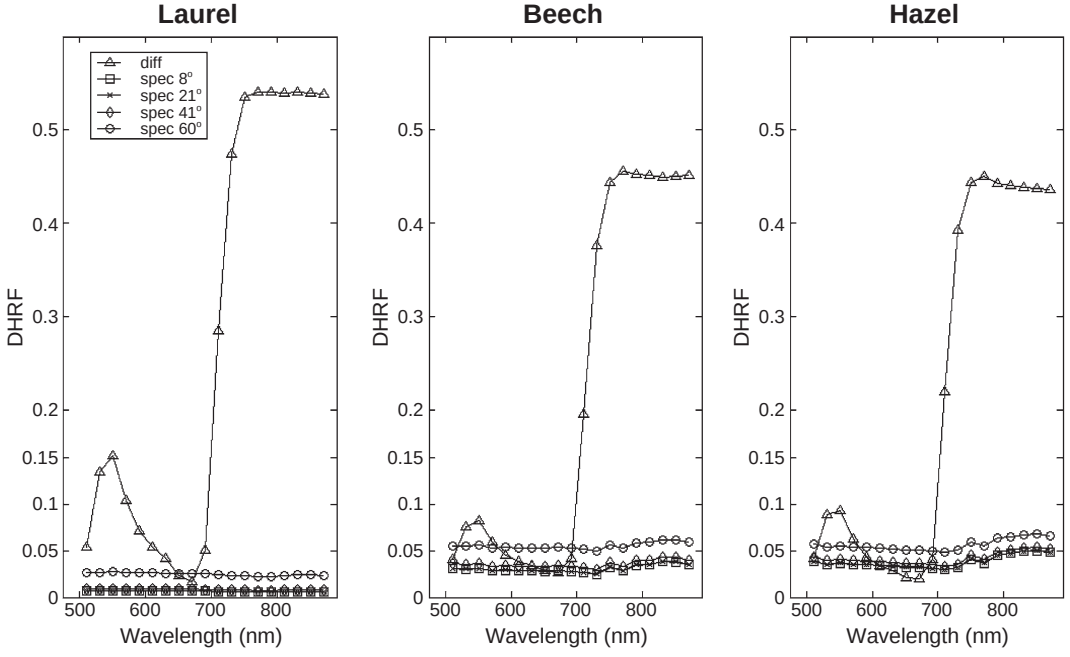

Fig. 6. Estimated diffuse and specular contributions to the DHRF for laurel (left), beech (middle), and hazel (right). Specular contribution is plotted for illumination angles θ_s=8°, 21°, 41°, and 60° (diffuse contribution is the same whatever the illumination angle).

Table 4
Mean leaf surface characteristics estimated in the 480–880 nm range

	Refractive index n	Roughness parameter σ
Laurel	1.22	0.078
Beech	1.56	0.29
Hazel	1.68	0.46

4.4. Evaluation of the amount of light that did not penetrate into the leaf

The retrieved model parameters are then used to estimate the diffuse and specular contributions to the DHRF at each wavelength:

$$\mathrm{DHRF}(\theta_s,\lambda) = \mathrm{DHRF}_{\mathrm{diff}}(\theta_s,\lambda) + \mathrm{DHRF}_{\mathrm{spec}}(\theta_s,\lambda) \quad (12)$$

with:

$$\begin{aligned}&\mathrm{DHRF}_{\mathrm{diff}}(\theta_s,\lambda)\\ &= \int_0^{2\Pi}\int_0^{\Pi/2} \mathrm{BRDF}_{\mathrm{diff}}(\lambda,\theta_s,\theta_v,\varphi_v)\cos\theta_v\sin\theta_v d\theta_v d\varphi_v\\ &= k_L(\lambda)\end{aligned} \quad (13)$$

$$\begin{aligned}&\mathrm{DHRF}_{\mathrm{spec}}(\theta_s,\lambda)\\ &= \int_0^{2\Pi}\int_0^{\Pi/2} \mathrm{BRDF}_{\mathrm{spec}}(n(\lambda),\sigma(\lambda),\theta_s,\theta_v,\varphi_v)\\ &\quad\times\cos\theta_v\sin\theta_v d\theta_v d\varphi_v.\end{aligned} \quad (14)$$

$\mathrm{DHRF}_{\mathrm{spec}}$ was numerically computed with a relative error below 10^{-4}. Fig. 6 shows both contributions for the four incidence angles θ_s. The specular contribution varies very slowly with the wavelength, whatever the leaf and the incidence angle. It is almost the same for θ_s=8°, 21° and 41° and double at θ_s=60°. It can be higher than the diffuse one for wavelengths of strong absorption.

4.5. Perspective for the estimation of leaf surface properties

Although plant cuticle has been studied in detail by Martin and Juniper (1970), Cutler et al. (1982) or Kerstiens (1996), its optical or roughness properties have barely been measured. The mean values of the retrieved cuticle refractive index and roughness parameter from 480 to 880 nm are listed in Table 4. The roughness parameter is minimum ($\sigma \sim 0.078$) for laurel which has a thick cuticle, maximum ($\sigma \sim 0.46$) for hazel which has hairy faces, and intermediate ($\sigma \sim 0.29$) for beech which has an intermediate surface structure. This result is consistent with our observations on fresh leaf materials. To the best of our knowledge, measured values for roughness of leaf surfaces have not been published so far. The refractive index follows the opposite variation: it is higher for hazel than for laurel. This can be explained by the high reflectance of hairy leaf even at low incidence angles. Hairs reflect light that has not interacted with the leaf interior and increase the apparent refractive index. Allen et al. (1969) give 1.47 for the refractive index of carnauba wax, a substance obtained from the leaf surface of *Capernicia cerifera* and Woolley (1975) proposes 1.48 for the living hairs of soybean leaves. In comparison the 1.22 value found for laurel is lower and those found for beech (1.56) and hazel (1.68) are higher. Various cuticle structures associated with an increase due to the presence of hair may explain such differences.

4.6. Perspective for a five-parameter leaf optical properties model using PROSPECT

In the above, the BRDF model requires three input parameters (k_L, n, and σ) at each wavelength, i.e., a total of $3\times400=1200$ parameters to simulate the full spectral and directional leaf optical properties in the VIS–NIR. This is neither convenient nor portable. We aim to reduce this number to only five. On the one hand, the refractive index n and roughness parameter σ have been shown to be almost wavelength independent in the VIS–NIR so that they can be replaced by their mean values. On the other

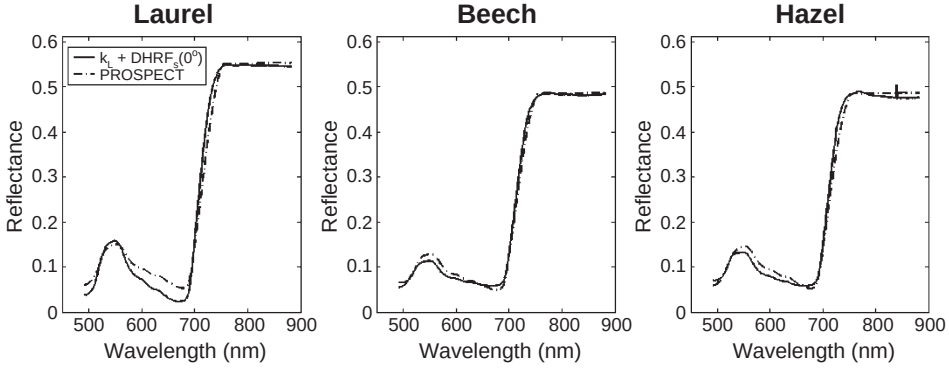

Fig. 7. DHRF (λ, 0°) simulated with the BRDF model (solid line) and fitted with the PROSPECT model (dashed line).

Table 5
Root mean square error (RMSE) between measured and modeled leaf BRDF

	RMSE ($k_L(\lambda)$, $n(\lambda)$, $\sigma(\lambda)$)	RMSE (n, σ, N, C_{ab}, C_m)
Laurel	1.51 10^{-2}	1.70 10^{-2}
Beech	1.12 10^{-2}	1.17 10^{-2}
Hazel	0.90 10^{-2}	1.01 10^{-2}

hand, the Lambert parameter $k_L(\lambda)$ which is strongly correlated with the leaf DHRF(λ) can be related to the PROSPECT model. The latter is used to simulate leaf hemispherical reflectance and/or transmittance and accounts for both specular and diffuse reflections, assuming that the illumination direction is normal to the leaf blade. Thus the reflectance $R_{prospect}$ simulated by PROSPECT should be equivalent to DHRF ($\lambda, \theta_s=0°$). The parameters required to run it in the VIS–NIR are the leaf structure parameter N (which ranges from 1 to 1.5 for monocots and from 1.5 to 2.5 for dicots), the chlorophyll a+b content C_{ab} (μg cm^{-2}) and the dry matter content C_m (g cm^{-2}). This yields to:

$$R_{prospect}(N, C_{ab}, C_m) = \mathrm{DHRF}(\lambda, 0°). \quad (15)$$

By evaluating Eq. (12) for $\theta_s=0°$ one has:

$$R_{prospect}(N, C_{ab}, C_m) = \mathrm{DHRF}_{diff}(\lambda, 0°) + \mathrm{DHRF}_{spec}(\lambda, 0°). \quad (16)$$

From Eq. (13) DHRF_{diff} is equal to $k_L(\lambda)$ for all θ_s. Because n and σ are approximated by their mean values, DHRF_{spec} is independent of the wavelength so that Eq. (16) may be written as:

$$R_{prospect}(N, C_{ab}, C_m) = k_L(\lambda) + \mathrm{DHRF}_{spec}(0°). \quad (17)$$

Finally, extracting k_L in Eq. (17) and substituting in Eq. (4) leads to a new expression for the BRDF model, the parameters of which are now wavelength independent:

$$\mathrm{BRDF}(\lambda, \theta_s, \theta_v, \varphi_v) = \frac{R_{prospect}(N, C_{ab}, C_m) - \mathrm{DHRF}_{spec}(n, \sigma, 0°)}{\pi} + \mathrm{BRDF}_{spec}(n, \sigma, \theta_s, \theta_v, \varphi_v). \quad (18)$$

We tested the ability of this five-parameter model to fit our measured BRDF. Since a global inversion of Eq. (18) led to instabilities on the retrieval of the PROSPECT parameters, we decided to calculate the mean value of n and σ (Table 4) and then to estimate the PROSPECT parameters by inverting Eq. (17). The fit of PROSPECT is very satisfying as shown in Fig. 7. To compare this five-parameter model with the previous version using 3×400 input parameters, we computed the root mean square error (RMSE) between the measured and modeled BRDF. Values gathered in Table 5 correspond to 4 illumination directions by 65 viewing directions by 400 wavelengths. The slight increase of the RMSE proves the effectiveness of our approach consisting of coupling PROSPECT with the BRDF model to simulate both the spectral and bidirectional reflectance of plant leaves.

5. Conclusion

Accurate leaf BRDF measurements were carried out for laurel, beech and hazel. These three species exhibit various BRDF shapes mainly due to the specular reflection influenced by leaf surface characteristics. The new goniometer enabled us to record the BRDF shape as a continuous function of the wavelength in the 480–880 nm range. Therefore, it was possible to show that the specular peak in laurel BRDF was almost independent of the wavelength. Then a BRDF model expressed as the sum of a diffuse and a specular component was used to fit the BRDF measurements. The parameters controlling the specular component were found to be almost independent of wavelength for each of the three leaf types. The model also permitted the evaluation of the proportion of diffuse and specular reflection at each wavelength. Finally, we associated this model with PROSPECT and reduced the number of parameters to only five: n (refractive index of leaf surface material), σ (surface roughness parameter), N (leaf structure parameter) and the biochemical contents C_{ab} (chlorophyll) and C_m (dry matter). The comparison of some of these parameters with the leaf biophysical characteristics, e.g., its biochemical composition or surface anatomical structure, would be required to completely validate the model. A laboratory experiment will soon bridge this gap.

As PROSPECT is widely used to estimate leaf biochemical compounds from hemispherical reflectance measurements, we wish to extend such estimates to directional measurements. Considering the leaf blade as an anisotropic surface instead of a Lambertian one, especially at orientations close to the specular direction, will change our perception of leaf optical properties, which has many significant underlying applications in plant physiology, computer-generated images, and vegetation remote sensing. For instance, the model will allow plant canopy reflectance modelers to test the validity of the argument that leaf BRDF is a minor factor in determining canopy reflectance.

Acknowledgements

This work was supported by the Programme National de Télédétection Spatiale (PNTS) and by the GDR 1536 FLUOVEG (Fluorescence of Vegetation). We are grateful to the three anonymous reviewers for their comments and recommendations. Many thanks to Susan Ustin for reading and correcting this paper.

References

Allen, W. A., Gausman, H. W., Richardson, A. J., & Thomas, J. R. (1969). Interaction of isotropic light with a compact plant leaf. *Journal of the Optical Society of America*, *59*, 1376–1379.

Baranoski, G. V. G., & Rokne, J. G. (2004). *Light interaction with plants. A computer graphics perspective*. Chichester: Horwood Publishing. 140 pp.

Brakke, T. W. (1994). Specular and diffuse components of radiation scattered by leaves. *Agricultural and Forest Meteorology*, *71*, 283–295.

Brakke, T. W., Smith, J. A., & Harnden, J. M. (1989). Bidirectional scattering of light from tree leaves. *Remote Sensing of Environment*, *29*, 175–183.

Breece, H. T., & Holmes, R. A. (1971). Bidirectional scattering characteristics of healthy green soybean and corn leaves in vivo. *Applied Optics*, *10*, 119–127.

Combes, D. (2002). Comparaison de modèles de transferts radiatifs pour simuler la distribution du rayonnement actif sur la morphogénèse (MAR) au sein d'un peuplement végétal à l'échelle locale. Thèse de Doctorat en Physique de l'Atmosphère Université Blaise Pascal. 175 pp.

Cook, R. L., & Torrance, K. E. (1981). A reflectance model for computer graphics. *Computer Graphics*, *15*, 307–316.

Cutler, D. F., Alvin, K. L., & Price, C. E. (Eds.). (1982). *The plant cuticle*. New York: Academic Press.

Fuhrer, M., Jensen, H. W., & Prusinkiewicz, P. (2004). Modeling hairy plants. *Proc. 12th pacific conference on computer graphics and applications* Seoul, Korea, 6–8 October 2004.

Govaerts, Y., Jacquemoud, S., Verstraete, M. M., & Ustin, S. L. (1996). Three-dimensional radiation transfer modeling in a dicotyledon leaf. *Applied Optics*, *35*, 6585–6598.

Jacquemoud, S., & Baret, F. (1990). PROSPECT: A model of leaf optical properties spectra. *Remote Sensing of Environment*, *34*, 75–91.

Juniper, B. E., & Jeffree, C. E. (1983). *Plant surfaces*. London: Edward Arnold 93 pp.

Kerstiens, G. (Ed.). (1996). *Plant cuticles: An integrated functional approach*. Oxford, UK: BIOS Scientific Publishers Limited.

Martin, J. T., & Juniper, B. E. (1970). *The cuticles of plants*. London: E. Arnold. 347 pp.

Nicodemus, F. E., Richmond, J. C., Ginsberg, I. W., & Limperis, T. (1977). Geometrical consideration and nomenclature for reflectance. *NBS Monograph.* NBS MN-160. 52 pp. October 1977.

Oren, M., & Nayar, S. K. (1995). Generalization of the Lambertian model and implications for machine vision. *International Journal of Computer Vision*, *14*, 227–251.

Torrance, K. E., & Sparrow, E. M. (1967). Theory for off-specular reflection from roughened surfaces. *Journal of the Optical Society of America*, *57*, 1105–1114.

Vanderbilt, V. C., & Grant, L. (1986). Polarization photometer to measure bidirectional reflectance factor *R* (55°, 0°; 55°, 180°) of leaves. *Optical Engineering*, *25*, 566–571.

Walter-Shea, E. A., Norman, J. M., & Blad, B. L. (1989). Leaf bidirectional reflectance and transmittance in corn and soybean. *Remote Sensing of Environment*, *29*, 161–174.

Ward, G. J. (1992). Measuring and modeling anisotropic reflection. *Computer Graphics*, *26*, 265–272.

Woolley, J. T. (1971). Reflectance and transmittance of light by leaves. *Plant Physiology*, *47*, 656–662.

Woolley, J. T. (1975). Refractive index of soybean leaf cell walls. *Plant Physiology*, *55*, 172–174.

Wylie, R. B. (1943). The role of the epidermis in foliar organization and its relations to the minor venation. *American Journal of Botany*, *30*, 273–280.